Simultaneous EUV and Optical Observations of the Magnetic Cataclysmic Variable PQ Geminorum

Steve B. Howell

Department of Physics and Astronomy, University of Wyoming

University Station, Laramie, WY 82071

Martin M. Sirk

Center for Extreme Ultraviolet Astrophysics, 2150 Kittredge Street

University of California, Berkeley, CA 94720

Gavin Ramsay

Astronomical Institute, Utrecht University

Postbus 80000 3508 TA Utrecht, The Netherlands and

University College London, Mullard Space Science Laboratory

Dorking, Surrey RH5 6NT, UK

Mark Cropper and Stephen B. Potter

University College London, Mullard Space Science Laboratory

Dorking, Surrey RH5 6NT, UK

Simon R. Rosen

Department of Physics and Astronomy, University of Leicester

University Rd., Leicester, UK LE1 7RH

Submitted to *Astrophysical Journal*

Received ________________________; accepted ________________________

ABSTRACT

We present the results of simultaneous optical polarimetry and EUV spectroscopy and photometry of PQ Gem, a magnetic cataclysmic variable which shows observational properties of the strongly magnetic AM Her class, as well as the weaker field DQ Her stars. The EUV spectrum of PQ Gem is weak, showing continuum blueward of 80 Å and a few possible weak emission lines due to Mg, Si, and Ne. The EUV lightcurve has a similar appearence to previous X-ray data obtained for PQ Gem, including a narrow "dip" feature which is modulated with the white dwarf spin period. Observed polarisation variations on the spin period, modelled by a slightly modified version of that used in Potter et al. (1997), matched the optical light curve and linear polarisation curve reasonably well, but not the position angle variation. The EUV properties of PQ Gem can also be understood in the context of this model.

Subject headings: Cataclysmic Variables, Magnetic CVs, Stars-individual:PQ Gem

1. Introduction

Magnetic cataclysmic variables (CVs) are divided into two classes—the DQ Her stars and the AM Her stars. The major distinction between these classes is the degree of synchronous rotation of the primary star, which is mainly dependent on its magnetic field strength and on the binary separation. In AM Her systems the field strengths are generally higher than 10 MG which is sufficient to disrupt any accretion disk, so that accretion takes place directly from the accretion stream. The DQ Her systems generally have weaker fields (1-10 MG where they can be inferred) and the material lost from the secondary may form a partial disk, which is disrupted at some point allowing material to accrete onto the white dwarf in large arcs or curtains. The white dwarf in DQ Her stars generally rotates faster than the binary orbital period, producing beat frequency variability in most wavebands.

Magnetic CVs are good targets for high-energy and polarization observations as modulation of the accretion flux occurs at the spin period, and additionally in the DQ Hers, at a number of frequencies, principally the white dwarf spin period and/or the spin-orbit beat period. Cropper (1990) provides a review of the AM Her variables while the DQ Hers are discussed in Patterson (1994) and Warner (1995).

PQ Gem (RE0751+14) was discovered in the *ROSAT* all-sky survey (Mason et. al. 1992). It was soon realized that this star was not a typical magnetic CV in that it could not be placed uniquely into the AM Her or the DQ Her catagory. In common with DQ Her systems, PQ Gem has an asynchronously spinning white dwarf (P_{spin} = 13.9 min; much shorter than its orbital period of 5.2 hrs), a strong spin-modulated hard X-ray pulse, and optical variations modulated on the beat frequency. However, it also shows spin modulated polarization and a photometric orbital variation in the red part of the optical spectrum. These latter features are typical of AM Hers and indicate a luminous cyclotron spectral component and a magnetic field strength stronger then in typical DQ Hers. Also, unusually for a DQ Her system, PQ Gem has a soft X-ray (EUV) component whose flux is modulated with the spin period and contains a narrow "dip" feature. These dip features are seen quite often in the X-ray light curves of AM Her stars (cf. Watson et al. 1989) and are attributed to the obscuration of the accretion region by the gas stream very near the white Dwarf surface.

Details of previous observations of PQ Gem can be found in Rosen et. al. (1993), Piirola, Hakala & Coyne (1993), Mason (1995), Stavroyiannopoulos et. al. (1997) and Potter et al. (1997).

2. Observations

2.1. *EUVE* Observations

The *EUVE* satellite performs simultaneous spectroscopic and photometric observations in the EUV spectral range (70 – 170 Å; Bowyer and Malina 1991, Sirk et al. 1997). The principle instrument on board consists of a telescope which contains an imager and three seperate spectrographs covering the total range of 70 – 750Å. The bandpass of the imager is set by the Lexan/Boron filter, with a maximum transmission at 91 Å with a 90% bandpass of 67 – 178 Å. The imager allows for collection of photometric data simultaneously with the spectroscopic data. The collected photons are position and time tagged providing very good time-resolution and allowing the production of detailed lightcurves (eg., Sirk and Howell 1995, 1997).

PQ Gem was observed with *EUVE* during 1996 Jan from 13 (10:34 GMT) to 19 (23:22 GMT); covering 30 binary orbits and 660 white dwarf spin periods. During the observations, it was detected with a mean count rate of 0.07 cts/sec in the imager. The *EUVE* spectral data were extracted and reduced to phased-resolved 2-D images as described in the *EUVE* users manual, and then to 1-D spectra as discussed in Hurwitz et al. (1996). The photometric data reduction proceeded as described in Howell et al. (1995). Figure 1 presents the short wavelength spectrum of PQ Gem divided into "bright" ($\phi_{spin} = 0.13 - 0.35$) and "faint" ($\phi_{spin} = 0.35 - 0.13$) phases of the spin period, and Figure 2 shows the photometric time-series lightcurve. The top panel shows the time-series data phased on the white dwarf spin period using the ephemeris

$$T(HJD) = 2448173.95714(5) + 0.0096458718(10)N + 5.24(4) \times 10^{-13}N^2$$

given in Mason (1997), while the bottom two panels of Fig. 2 phase the EUV photometry on the spin-orbit beat period and the binary orbital period, (see Stavroyiannopoulos et. al. 1997).

2.2. Optical Observations

Optical observations were obtained during 1996 Jan 15–17 using the EFOSC2 instrument together with a Thomson 1024 x 1024 CCD as the detector on the ESO/MPI 2.2m telescope at La Silla, Chile. Integration times of 30 sec were used with a 34 sec deadtime. The conditions were photometric with seeing typically 1.0–1.5$''$. A Wollaston prism was used to produce 2 images of the object on the CCD. No quarter wave plate was available so only linear polarisation measurements were possible. As PQ Gem is polarised most strongly towards red wavelengths (cf. Potter et al. 1997), we used a Gunn i filter which has a peak transmission at 7600Å and a passband between 7200–8600Å (FWHM). Observations of polarised and non-polarised standards were made during the 3 nights to remove instrumental polarisation.

Aperture photometry was used to obtain light curves of PQ Gem through o and e rays. Care was taken to exclude the light from a faint star $3.6''$ from PQ Gem. The background-subtracted light curve is shown in Figure 3. The spin period of the white dwarf (833.4 secs) and the binary orbital period (5.2 hrs) are clearly seen in the lightcurve and in the power spectrum (Figure 4).

One Stokes parameter is measured for each particular orientation of EFOSC2. Depending on the position angle variation of the polarisation vector, the observed power can be different in the Stokes U and Q parameters. Since the rotator could not be moved remotely, we were prevented from obtaining quasi-simultaneous measurements of both Q and U Stokes parameters. Measurements of PQ Gem were made at one rotator angle for a half or whole night before rotating the instrument through 45°. We have therefore relied on averaging of the spin phase-resolved lightcurve to construct the linear polarizations.

3. Results

3.1. EUV Results

3.1.1. EUV Spectrum

The EUV spectrum of PQ Gem (Fig. 1) reveals essentially no continuum emission longward of $\sim$ 90 Å. Fluxes shortward of 73 Åare too close to the detector edge to be reliable. In the range of $75 - 90$ Å we find what may be weak emission features; however, they are only 1σ detections. The lines could be due to Mg VIII (74.8 & 75 Å), Si VI (80.5 Å), and Ne VI (85 Å) with the faint phase spectrum revealing that possibly the Si VI line becomes stronger, Ne VI weakens, and Mg VI/Si VI (83 & 83.1 Å) is present. The S/N of the spectrum is too low to allow any reliable fitting to be performed. Using the EUV emission line data provided in Mewe et. al., (1986) and attempting to find a single temperature which could account for all the possible lines, the emission line ratios can be used to roughly infer an emission region temperature of log T = 5.8-6.0 K.

The relatively weak emission line spectrum of PQ Gem contrasts with that of the only other DQ Her star yet observed with *EUVE*, EX Hya, which shows a spectrum dominated by Fe emission lines and can be fitted with an optically thin spectrum with log T = 7.0 K (Hurwitz et al. 1996). On the other hand, AM Her, with a field strength of 13 MG, shows a short wavelength EUV spectrum possibly containing some weak short wavelength emission lines, with a best continuum fit model of log T = 5.4 K (Paerels et al. 1996). PQ Gem, with a magnetic field at the interface of these two classes of magnetic CV, (8-18 MG (Piirola et al. 1993), therefore appears to have an EUV spectrum spanning the two groups as well. Assuming the same absorbing column to the source of 1.7×10^{20} cm^{-2} as Mason (1995), we find that the spectral flux of PQ Gem at 100Å is consistent with the previously measured *ROSAT* soft X-ray flux.

In both PQ Gem and EX Hya, the spectrum presented and used for analysis is a summation (for sufficient S/N) over many white dwarf spin periods. We note here that each of the bright and faint phase spectra in Fig 2 contain contributions from a number of regions at or near the white dwarf surface which differ in density and temperature. EUV spectroscopy with greater S/N and phase resolution will be necessary to disentangle the contributions from various temperature regions observed as the white dwarf spins.

3.1.2. EUV Photometry

The top panel in Fig. 2 clearly shows the modulation present in the EUV flux when phased on the white dwarf spin period. Duck et. al. (1994) and Mason (1995) show that a narrow dip occurs in the *ROSAT* PSPC X-ray light curve at the white dwarf spin period. The lightcurve in the top panel of our Fig. 2 is similar to that observed using *ROSAT*.

The dip in the PQ Gem X-ray lightcurve was used as a zero point for phasing the spin period in the Mason (1997) ephemeris used in Section 2.1. The bottom two panels show no significant modulation of the flux with either the beat or the binary orbital period.

Using HST/FOS spectra covering 1000-2500 Å, Stavroyiannopoulos et. al. (1997) saw evidence for a similar, yet broader dip in the blue continuum region which was offset in phase from the X-ray dip by 0.08 ± 0.02 in phase, or 67 sec. They interpreted this phase delay as due to the reprocessing of high-energy photons emitted from the hot accretion regions near the white dwarf surface by the outer accretion stream or curtain regions. These same authors also find that the 'blue' flux (summation of spectral flux from 1270-1460 Å, minus any emission lines present) was modulated on the white dwarf spin while the 'red' continuum (1800-2505 Å) was modulated on the spin-orbit beat, but not on the spin period itself. Our EUV light curve also shows this narrow dip feature with a width smaller than in the UV, similar to that seen in X-ray data. Using the ephemeris given above, we find that the dip centroid is not coincident with $\phi_{spin} = 0.0$, but is offset in phase by 0.03 or 26.19 ± 30.93 sec. The large uncertainty in the dip phase is based on the fact that nearly 200,000 spin periods have passed since the epoch of the ephemeris, allowing the error to accumulate. Given the greater delay seen in this feature in the UV data taken at an earlier epoch than the EUV data, we hesitate to use our EUV data to refine the ephemeris. However, if the reader wishes to do so we have provided an averaged timing for the dip in Fig. 2.

3.2. Polarisation Results

To determine the optical spin period behaviour we fitted a polynomial to the time series data to remove the effects of the orbital period. We then folded and binned the 4 light curves (o and e ray data through 2 rotator angles) on the white dwarf spin ephemeris of Section 2. (This assumes that the polarisation curve is broadly repeatable from orbit to orbit: typical of AM Her systems). The mean folded light curve, mean linear polarisation curve, and position angle are shown in Figure 5. The mean light curve in Figure 5 is similar to that shown in Mason (1995) in that it shows two peaks with the brightest occuring at $\phi_{spin} = 0.45$ and the secondary peak occuring at $\phi_{spin} = 0.9$, the same phase as the X-ray dip.

For the AM Her systems the interstellar component of the measured polarisation is typically negligible compared to their intrinsic polarisation and so this component is ignored. However, for weakly polarised sources the effect of the interstellar polarisation has to be considered. Mathewson & Ford (1970) give maps of interstellar polarisation as a function of galactic co-ordinates. PQ Gem has galactic co-ordinates $l = 203°$ and $b = 11.5°$. There are 4 stars near this position: HD65803, HD65970, HD66665 and HD68439. The mean angle of the linear polarisation is 48°, while using the 2 stars with linear polarisation above 0.1%, we find a mean linear polarization of 0.2% at 50°. We thus subtracted an interstellar linearly polarised component of 0.2% at 50° from the Q and U parameters to give the intrinsic polarised component of PQ Gem. The light curves, linear polarised curves, and position angle curves with the interstellar component subtracted are also shown in Figure 5.

The folded light curve obtained from the optical polarimetry presented here is similar to that shown in Piirola et al. (1993). However, the linear polarization data are very different. Piirola et al.'s linear data (the only other linear polarimetry data on PQ Gem), yields a peak in linear polarisation near $\phi_{spin} = 0.45$ while our data show a minimum. Further, these authors linear polarization position angle varies quite smoothly over 180° while ours is approximately constant at 50–60°.

Using the linear polarised versus distance relation of Barrett (1996) results in a distance for PQ Gem of 220pc [1]. This estimate is subject both to the uncertainty in our value for the interstellar polarisation and also the uncertainty in the Barrett relation. These are difficult to establish, but we estimate the uncertainty in the distance to be $\sim\ \pm$ 80pc.

4. Discussion

We have seen that the EUV spectrum of PQ Gem is unremarkable, revealing the possible presence of only a few weak emission lines. These data, while not conclusive, are consistant with a mean accetion region temperature of log T = 5.8-6.0 K (Mewe, Lemen & van den Oord 1986, Monsignori-Fossi & Landini 1994). PQ Gem's overall spectral appearence and accretion region temperature place PQ Gem squarely in the middle ground between the AM Her and the DQ Her stars, a position which PQ Gem has occupied since its discovery independent of the waveband of observation.

The white dwarf spin-phased lightcurve (Fig 2) reveals roughly three distinct regions: a rapid rise to a bright phase immediately following the dip ($\phi_{spin} = 0.0 - 0.17$); a slower decline region ($\phi_{spin} = 0.17 - 0.65$); and a roughly constant faint phase ($\phi_{spin} = 0.65 - 0.0$).

The EUV dip corresponds to the phase when the accretion region is obscured by the accretion stream (cf Potter et al 1997). The duration of the dip, $\sim$ 40 sec, provides a measure of the size of the near-surface stream. This well confined part of the accretion stream (or at least the EUV scattering region) near the white dwarf surface is $\sim$ 1000 km in width if the apparent spot latitude is 65° (see below). This is similar to the soft X-ray result obtained for PQ Gem by Duck et al. (1994) and matches well with accretion spot sizes found from EUV data for other AM Hers (Sirk and Howell 1995, 1997, Hurwitz et al.

[1]Note, in Barrett's paper there is an error in the P/d relation for $b > 10°$: it should be $P/d = 0.9$, not 0.7

1996).

Epoch-dependent changes in the stream geometry and thus impact site may be the cause of the slight phase offsets seen for the EUV dip noted above and possibly those shown to be present in the UV as well. Changes in the size, shape, and brightness centroid of the accretion spot with time have been seen in EUV photometric data for the AM Her stars RE1149+28 (Howell et al. 1995) and UZ For (Sirk & Howell 1997).

We began our interpretation of the polarisation data by considering whether the polarisation minima at $\phi_{spin} = 0.45$ and 0.85 could simply be the result of depolarisation (the linear polarisation curve is almost a mirror image of the flux curve). However, this is unlikely given that the fractional peak-to-minimum variation in the flux is only ~ 0.1, whereas the change polarisation is significantly greater, even when the interstellar polarisation component is not removed.

We have therefore used a model for PQ Gem developed in Potter et. al. (1997), with parameters modified as little as possible to fit our new data presented here. We have retained the two symmetrical accretion regions needed to account for the presence of both positive and negative circular polarisations. The Potter et al. (1997) model predicts a peak in linear polarisation at $\phi_{spin} = 0.5$, whereas our data require this to be shifted to $\phi_{spin} = 0.65$ to correspond to the broad maximum there. In addition the predicted linear polarisation around $\phi_{spin} = 1.0$ needs to be enhanced to match what we observe. The observed linear pulses are longer in time than would occur from small confined accretion regions. We find that by extending both accretion arcs along their length towards the equator (an increase in longitude by 20^{o} and in latitude by 30^{o} compared with the arcs used by Potter et al 1997), and enhancing the brightness of the ends of the arcs, it is possible to make an improvement to our fit (Fig 6). These stated modifications shift the peak in the model linear polarisation to $\phi_{spin} = 0.55$ and enhance the linear polarisation around

$\phi_{spin} = 0.2$. However, the model flux does not correctly reproduce the observed intensity peak at $\phi_{spin} = 0.9$. It is possible to further improve the fit at $\phi_{spin} = 0.9$ by the use of asymmetric arcs; however, this is probably not warranted by the data. Furthermore, our observed position angle is roughly constant at 50–60^{o}, while the model varies by $\sim 180^{o}$. We are unable to account for this.

Our model suggests that the first linear polarization pulse occuring near $\phi_{spin} = 0.6-0.8$, arises when the emission region in the upper hemisphere disappears over the limb of the white dwarf. Roughly simultaneously, the emission region from the lower hemisphere appears over the limb of the white dwarf. The second pulse is caused in a like manner but the emission regions are reversed.

The peak seen in our EUV photometry (~ 0.2 in phase; Fig 2) corresponds with a flux minimum as seen in the simultaneously obtained optical data (Fig 5). Our model indicates that the optical minimum seen at this phase is due to cyclotron beaming and scattering in the accretion region when seen nearly face on. The end of the slow decline in EUV flux at $\phi_{spin} = 0.5$ corresponds to the linear polarization peak as the region in the upper hemisphere passes over the limb. The majority of the EUV flux is therefore being emitted from the accretion region in the upper hemisphere which is visible during the EUV bright phase (noted above) between $\phi_{spin} = 0.1$ and 0.5 (see Potter et al. 1997, figure 9). The EUV decline phase occurs when the line of sight passes through the thinner trailing edge of the accretion curtain. The roughly constant faint phase is the time during which EUV emission is seen from the pole in the lower hemisphere.

In conclusion, PQ Gem appears to be a member of a new, small class of intermediate polars (DQ Her systems) which are strong soft X-ray emitters. Its EUV properties are intermediate between AM Her systems and intermediate polars. Other likely members of this group are RXJ0512-32 (Burwitz et al. 1996), RXJ0558+53 (Haberl et al. 1994), and

RXJ1914+24 (Haberl & Motch 1995). The polarisation of PQ Gem at the white dwarf spin period can be fitted to a certain extent by a slightly modified version of the model used in Potter et al (1997), but the reduced position angle variation remains unexplained. PQ Gem and the other three systems mentioned above, make up an interesting set of objects for further study in order to refine their complex properties.

The authors are grateful to the staff of the Center for Extreme Ultraviolet Astrophysics for their continued excellent work of running the *EUVE* satellite. We also want to thank the ESO director for the allocation of observing time as the support staff for their help. The anonymous referee made a number of useful suggestions which have improved the paper. SBH acknowledges support of this work by NASA grants S-14602-F and NAG 5-2989. GR would like to thank the European Union for a fellowship.

REFERENCES

Barrett, P., 1996, PASP, 108, 412

Bowyer, S., and Malina, R. F., 1991, in *Extreme Ultraviolet Astronomy*, eds. Malina & Bowyer, (New York;Pergamon), 397.

Burwitz, V., Reinsch, K., Beuermann, K., Thomas, H.-C., 1996, A&A 310, 25.

Cropper, M., Space Science Rev, 54, 195

Duck, S., Rosen, S., Ponman, T. J., Norton, A. J., Watson, M. G., & Mason, K. O., 1994, MNRAS, 271, 372.

Haberl, F. & Motch, C., 1995, A&A, 297, L37.

Haberl, F., Throstensen, J. R., Motch, C., Schwarzenberg-Czerny, A., Pakull, M., Shambrook, A., Pietsch, W., 1994, A&A, 291, 171.

Howell, S. B., Sirk, M. M., Malina, R. F., Mittaz, J. P. D., & Mason, K. O., 1995, Ap. J., 439, 995.

Hurwitz, M., Sirk, M., Bowyer, S., & Ko, Y., 1996, ApJ, in press.

Mason, K. O., et. al., 1992, MNRAS, 258, 749

Mason, K. O., 1995, in *Cape Workshop on Magnetic CVs*, ASP Conf. Series Vol. 85, eds. Buckley and Warner, p. 225.

Mason, K. O., 1997, MNRAS, in press.

Mathewson, D. S., & Ford, V. L., 1970, Mem. RAS, 74, 139

Mewe, R., Lemen, J. R., & van den Oord, G. H. J., 1983, A&A Suppl., 65, 511.

Monsignori-Fossi, B. C., & Landini, M., 1994, Sol. Phys. 152, 81.

Paerels, F., Hur, M. Y., Mauche, C. & Heise, J, 1995, ApJ, 464, 884

Patterson, J., 1994, PASP, 106, 209.

Piirola, V., Hakala, P. J., Coyne, S. J., 1993, Ap. J., 410, L107.

Potter, S. B., Cropper, M., Mason, K. O., Hough, J. H., & Bailey, J. A., 1997, MNRAS, in press.

Rosen, S. R., Mittaz, J. P. D., & Hakala, P. J., 1993, MNRAS 264, 171

Sirk, M. M., & Howell, S. B., 1995, in *Astrophysics in the Extreme Ultraviolet*, eds. Bowyer and Malina, (Kluwer), p 343.

Sirk, M. M., & Howell, S. B., 1997, in prep.

Sirk, M., M., Vallerga, J. V., Malina, R. F., Finley, D. S., & Jelinsky, P., 1996, submitted to ApJ.

Stavroyiannopoulos, D., Rosen, S. R., Watson, M. G., Mason, K. O., and Howell, S. B., 1997, MNRAS in press.

Warner, B. 1995a, Cataclysmic Variables Stars (Cambridge University Press, Cambridge), Chs. 3&9.

Watson, M. G., King, A. R., Jones, M. H., Motch C., 1989, MNRAS, 237, 299

Wickramasinghe, D. T. & Meggitt, S. M. A., 1985, MNRAS, 214, 605.

This manuscript was prepared with the AAS LaTeX macros v4.0.

Figure Captions

Figure 1. EUV Spectrum of PQ Gem. The spectrum shows a rising blue continuum shortward of ~ 90 Å with a few possible weak emission lines. The bright and faint phase summed spectra, (phase corresponds to that shown in Fig 2), essentially differ only in overall flux levels in both the continuum and the lines. The thin line running through the spectra is the 1σ uncertainty at each wavelength, based on counting statistics. These data are boxcar smoothed by 6 channels or 0.4 Å.

Figure 2. EUV lightcurve of PQ Gem showing (top to bottom), the data phased on the white dwarf spin period (using the epemeris given in the text), the spin-orbit beat period, and the binary orbital period. The data were binned as appropriate for the period search in each of the panels and have time bins of 3.35, 4.38, and 131.6 sec respectively, from top to bottom.

Figure 3. Optical, Gunn i filter, lightcurves of PQ Gem from ESO for our three nights of observation. The modulations due to the white dwarf spin period and the orbital period are clearly seen. The second and third nights observations have been displaced vertically by 700 and 1400 counts respectively for clarity.

Figure 4. Power spectrum of the ESO data for both the Stokes U and Q parameters. Both the white dwarf spin period (and harmonics) and the binary orbital period are visible in the U Stokes parameter power spectrum.

Figure 5. ESO polarimetry obtained with a Gunn i filter and phased on the white dwarf spin period, both before (left hand panel), and after (right panel) correction for instellar polarization (see text).

Figure 6. Model fits, based on a slightly modified version of the model developed in Potter et. al. (1997), overplotted on the optical data. We also show the predicted circular

polarisation for this model.

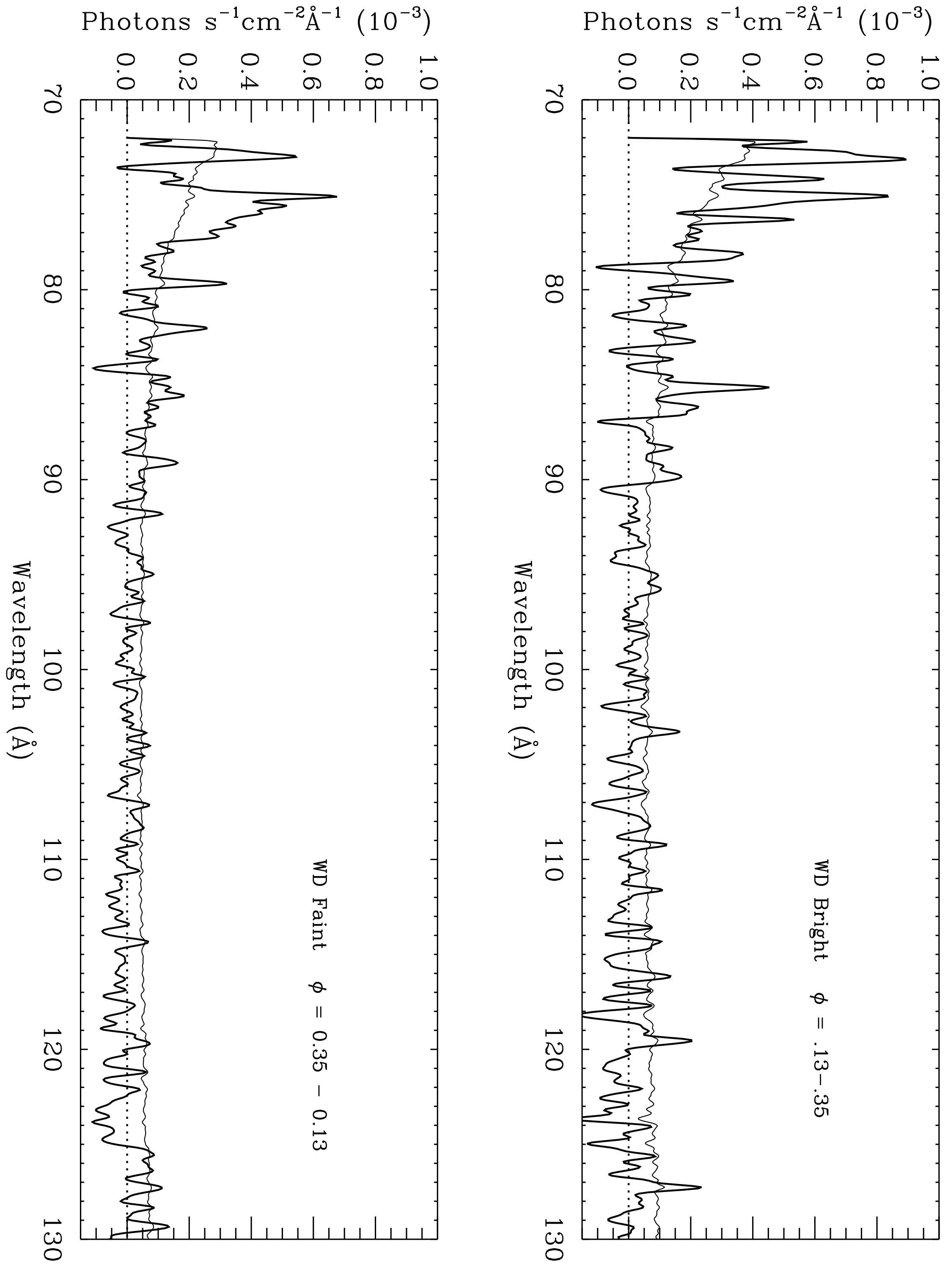

Photons s^{-1}cm^{-2}Å^{-1} (10^{-3})
Wavelength (Å)
WD Bright φ = .13–.35
Photons s^{-1}cm^{-2}Å^{-1} (10^{-3})
Wavelength (Å)
WD Faint φ = 0.35 – 0.13

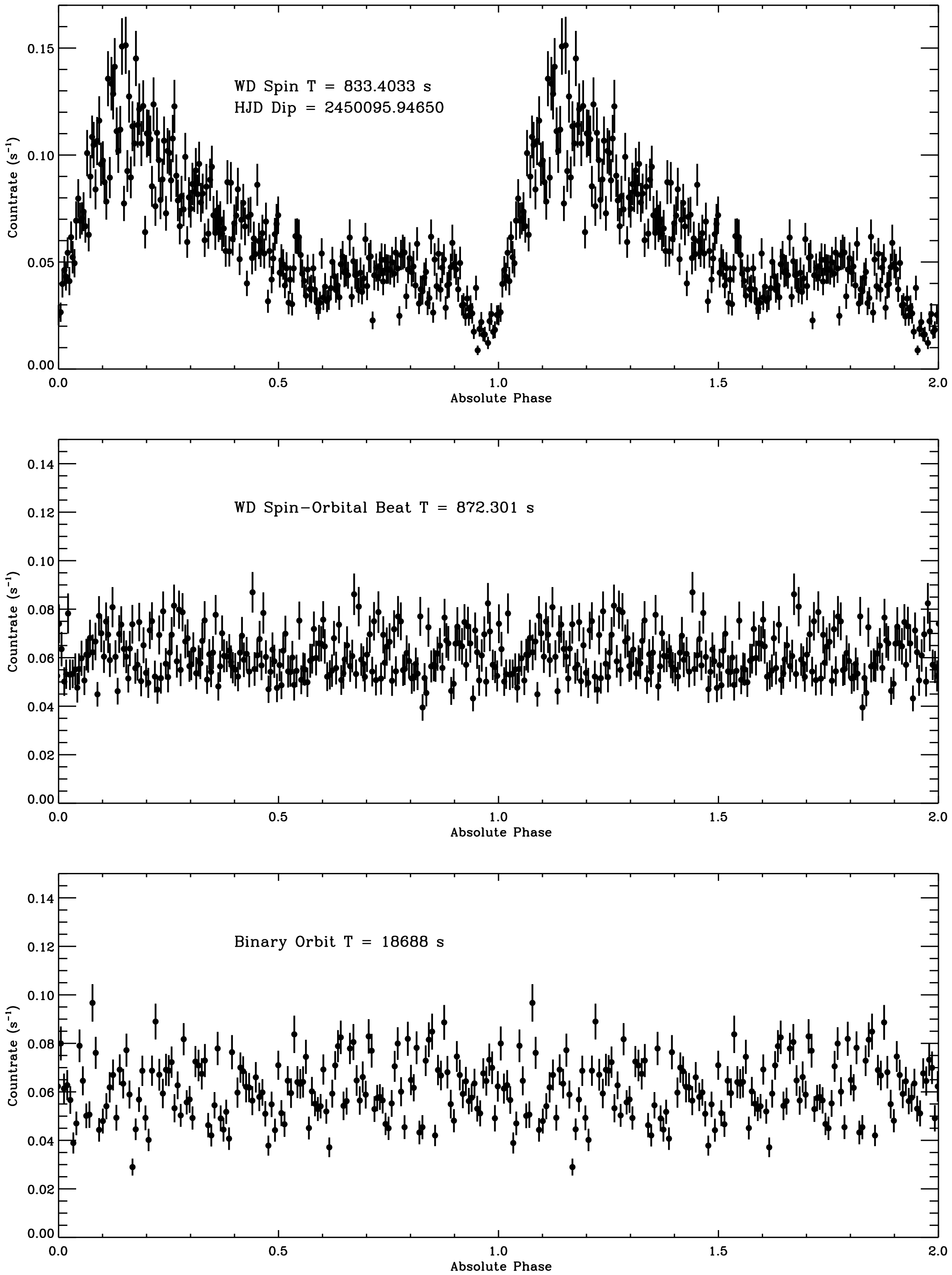
WD Spin T = 833.4033 s
HJD Dip = 2450095.94650
WD Spin−Orbital Beat T = 872.301 s
Binary Orbit T = 18688 s
Countrate (s⁻¹)
Absolute Phase
0.00
0.05
0.10
0.15
0.02
0.04
0.06
0.08
0.12
0.14
0.0
0.5
1.0
1.5
2.0

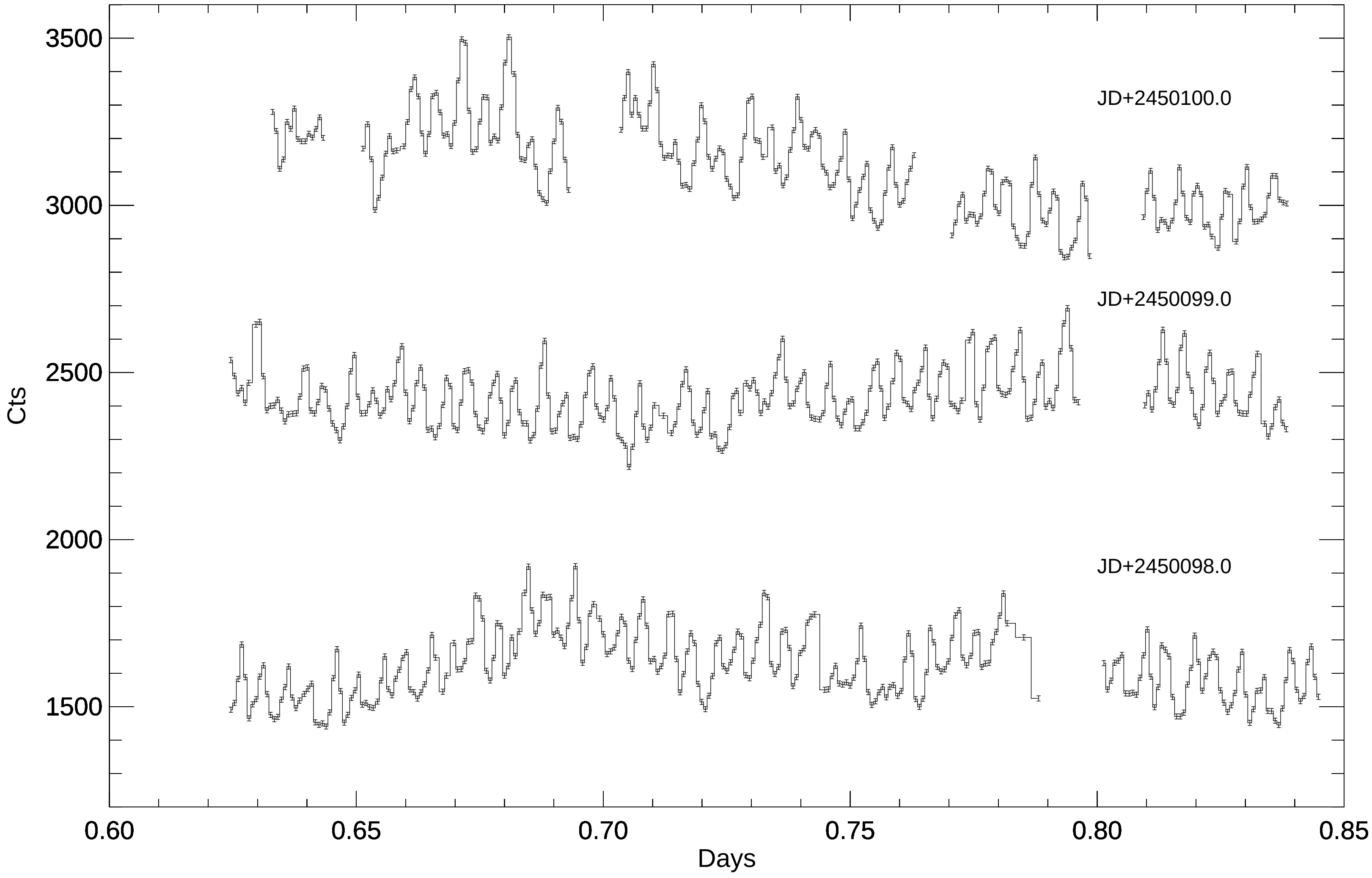
JD+2450100.0
JD+2450099.0
JD+2450098.0
Cts
3500
3000
2500
2000
1500
0.60
0.65
0.70
0.75
0.80
0.85
Days

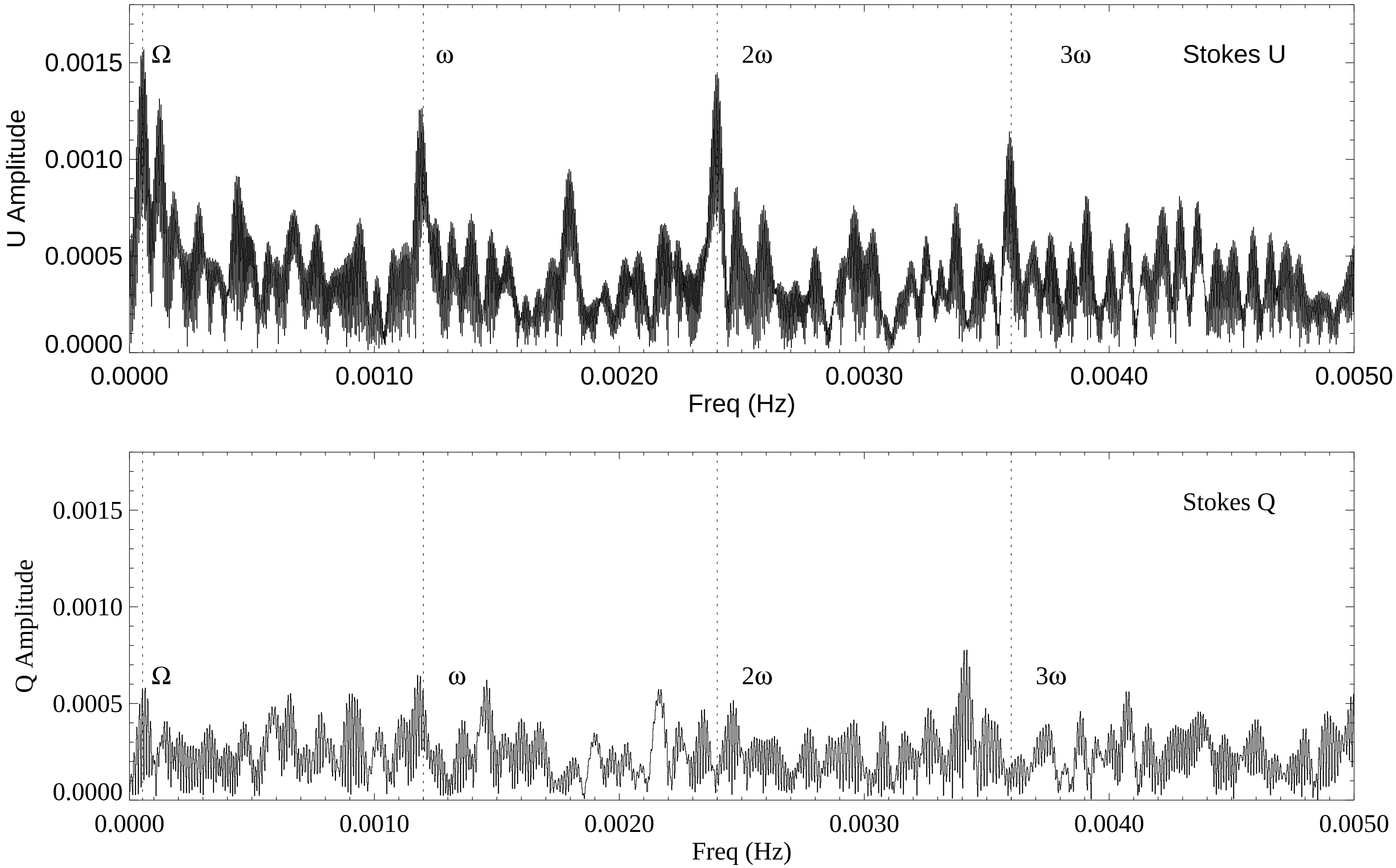

Stokes U
U Amplitude
Ω
ω
2ω
3ω
0.0000
0.0005
0.0010
0.0015
0.0000
0.0010
0.0020
0.0030
0.0040
0.0050
Freq (Hz)
Stokes Q
Q Amplitude
Ω
ω
2ω
3ω
0.0000
0.0005
0.0010
0.0015
0.0000
0.0010
0.0020
0.0030
0.0040
0.0050
Freq (Hz)

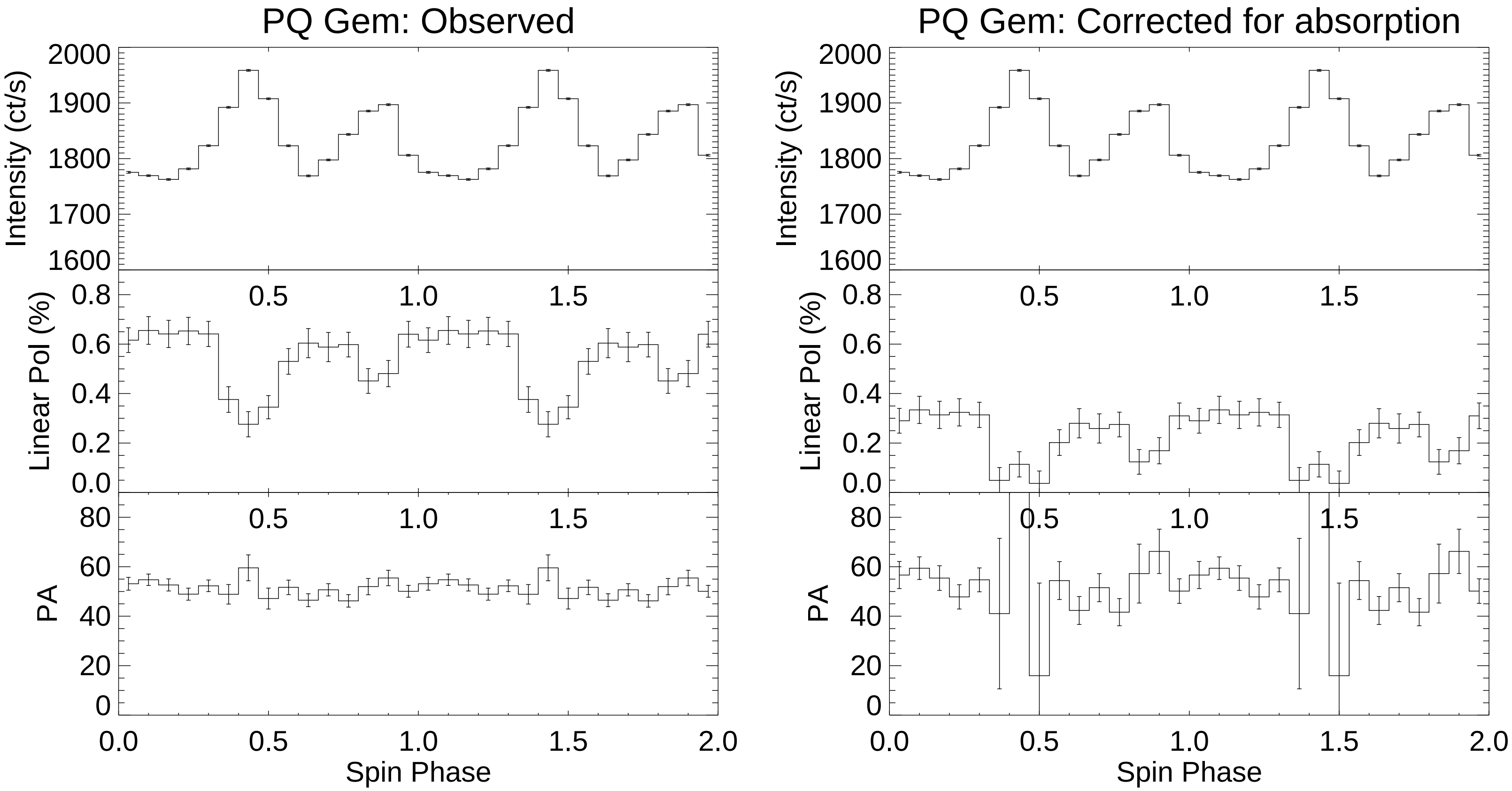

PQ Gem: Observed
PQ Gem: Corrected for absorption
Intensity (ct/s)
2000
1900
1800
1700
1600
Linear Pol (%)
0.8
0.6
0.4
0.2
0.0
PA
80
60
40
20
0
0.0
0.5
1.0
1.5
2.0
Spin Phase

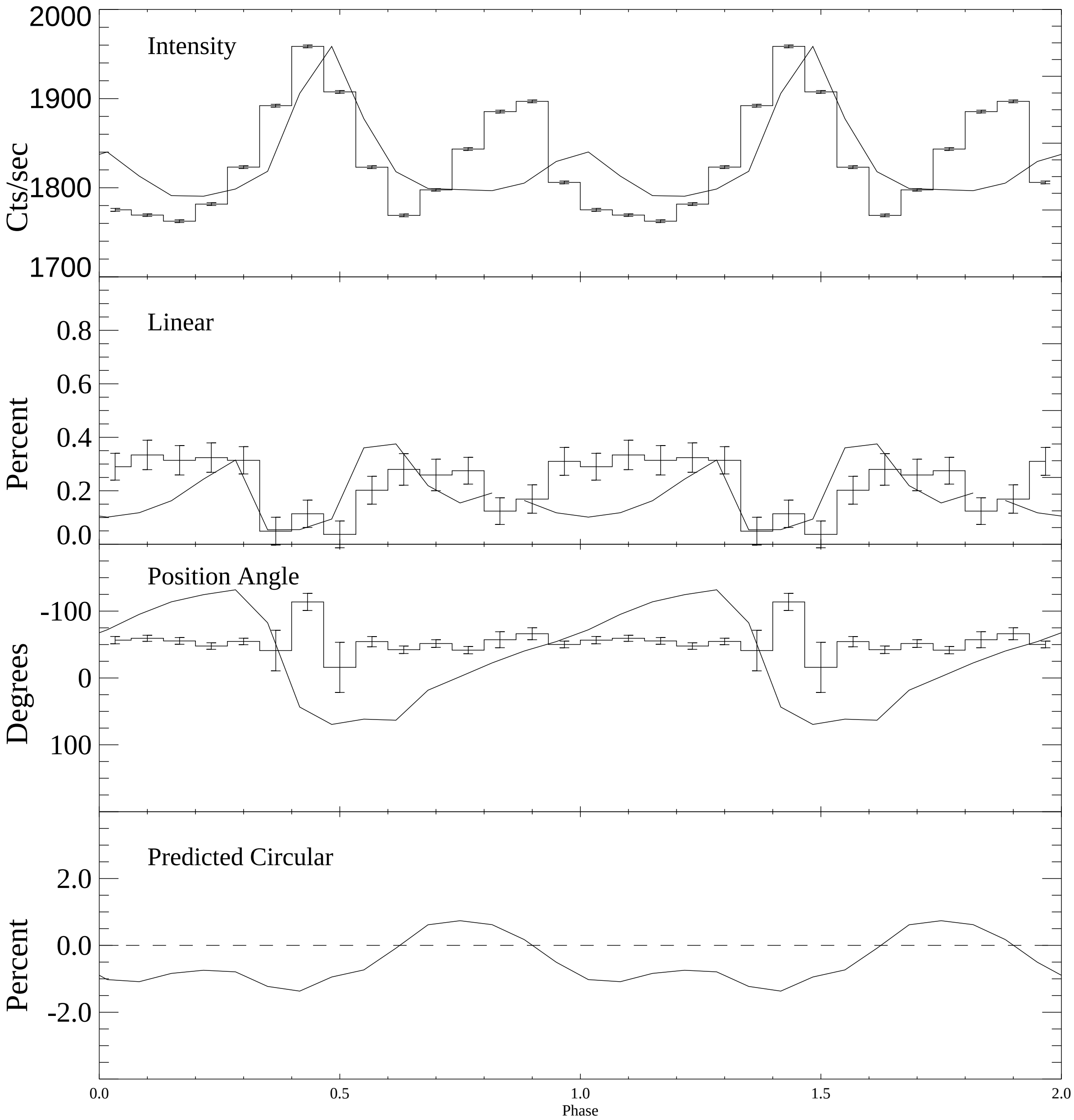

Intensity
Cts/sec
2000
1900
1800
1700
Linear
Percent
0.8
0.6
0.4
0.2
0.0
Position Angle
Degrees
-100
0
100
Predicted Circular
Percent
2.0
0.0
-2.0
0.0
0.5
1.0
1.5
2.0
Phase